



Contents lists available at ScienceDirect

International Communications in Heat and Mass Transfer

journal homepage: www.elsevier.com/locate/ichmt

Transportation of Marangoni convection and irregular heat source in entropy optimized dissipative flow

M. Ijaz Khan^a, Sumaira Qayyum^b, Yu-Ming Chu^{c,d,*}, Niaz B. Khan^e, Seifedine Kadry^f

^a Department of Mathematics and Statistics, Riphah International University, I-14, Islamabad 44000, Pakistan

^b Department of Mathematics, Quaid-I-Azam University 45320, Islamabad 44000, Pakistan

^c Department of Mathematics, Huzhou University, Huzhou 313000, PR China

^d Hunan Provincial Key Laboratory of Mathematical Modeling and Analysis in Engineering, Changsha University of Science & Technology, Changsha 410114, PR China

^e School of Mechanical and Manufacturing Engineering, National University of Sciences and Technology, Islamabad, Pakistan

^f Department of Mathematics and Computer Science, Beirut Arab University, Beirut, Lebanon

ARTICLE INFO

Keywords:

Marangoni convection, entropy generation
Rotating disk
MHD
Nonlinear mixed convection
Irregular heat source
Thermal radiation

ABSTRACT

This paper is about entropy generation in Marangoni convective flow due to rotating disk with irregular heat source. Nonlinear mixed convection radiative flow is considered here. Exponential base heat source is addressed. Subsequent equations are transformed to the ODE's by using generalized Karman's variables. Results are found by using NDSolve MATHEMATICA. Through graphical illustration velocity, temperature, Bejan number and entropy generation are discussed. Axial velocity enhances via Marangoni number while temperature decays. Velocity is greater via larger nonlinear thermal convection parameter. Entropy rate boosts up for variation of nonlinear convection parameter and Marangoni number. Bejan number decays against Brinkman number and nonlinear convection parameter.

1. Introduction

Marangoni effect means the mass transfer due gradient of surface tension between two fluids interface. It is also called thermo-capillary convection when it depends on temperature. In 1855 this mechanism is firstly introduce by James Thomson a physicist by "tears if wine." A region where surface tension is high strongly pull the surrounding fluid particles as compared to low surface tension region, so the gradient in the surface tension is the reason why liquid move from high surface tension to low surface tension. Gradient of surface tension is due to temperature or concentration gradient. There are many practical applications of Marangoni effect such as stabilization of soap films, Benard cell or convection cell etc. One of important application is that in production of integrated circuit it is used to dry the silicon wafer after a wet processing otherwise if liquid left on the surface of wafer can damage components due to oxidation. The Marangoni effect is also used in crystal growth, electron beam melting of metals and welding. Gangadharaiyah [1] discovered the superposed fluid flow with Marangoni convection. Sreenivasulu et al. [2] discussed the Marangoni convection flow with thermal radiation and Joule heating with heat and mass transfer. Mahanthesh and Gireesha [3,4] analyzed the Marangoni effect

on dusty Casson fluid radiative flow with Joule heating and viscous dissipation. Hayat et al. [5] worked on carbon-water nanofluid with Marangoni convection. More recent studies [5–10] in which Marangoni convection effect is studies in different situations.

Entropy rate in any irreversible process is known as entropy generation or production. There are many reasons due to which entropy generated such as heat exchange, mixing and expanding of substances, motion of bodies, fluid flow, solid deformation, or any irreversible thermodynamic cycle such as thermal machines e.g., heat pumps, air conditioners, heat engines, power plants etc. Due to irreversible processes entropy is generated some of them are (i) Diffusion (ii) Joule heating (iii) Chemical reactions (iv) flow of heat by thermal resistance (v) viscosity of the fluid (vi) friction of solid surfaces. Hayat et al. [11] examined the irreversibility in flow of copper and silver nanoparticles. Goqo et al. [12] analyzed the irreversibility over a porous wedge with thermal radiation and nanofluid. Khan et al. [13] worked on nano-material flow of fluid with irreversibility. Some more studies regarding this topic can be seen through refs. [14–22].

This paper is about entropy generation in Marangoni convective flow due to rotation of disk with irregular heat source. Nonlinear mixed convection radiative flow is considered here. Exponential base heat

* Corresponding author at: Department of Mathematics, Huzhou University, Huzhou 313000, PR China.

E-mail address: chuyuming@zjhu.edu.cn (Y.-M. Chu).

<https://doi.org/10.1016/j.icheatmasstransfer.2020.105031>

0735-1933/© 2020 Elsevier Ltd. All rights reserved.

source is addressed. Subsequent equations are transformed to the ODE's by using transformations. Graphs are drawn to see the behavior of fluid characteristic via interesting parameters.

2. Statement

Modeling is done for 3D, incompressible, steady Marangoni convective MHD flow due to rotating disk. Heat generation absorption effect is considered in heat equation with irregular heat source. Nonlinear mixed convection flow is considered here. Thermal radiation effect is also considered in heat equation. Exponential base heat source is addressed. Cylindrical model system is shown in Fig. 1. Under all these assumptions governing equations are

$$\frac{\partial u}{\partial r} + \frac{v}{r} + \frac{\partial w}{\partial z} = 0 \quad (1)$$

$$u \frac{\partial u}{\partial r} + w \frac{\partial u}{\partial z} = \frac{\mu}{\rho} \frac{\partial^2 u}{\partial z^2} - \frac{\sigma^*}{\rho} B_0^2 u + g[\beta_1(T - T_\infty) + \beta_2(T - T_\infty)^2] \quad (2)$$

$$u \frac{\partial T}{\partial r} + w \frac{\partial T}{\partial z} = \frac{k}{(\rho c_p)} \frac{\partial^2 T}{\partial z^2} + \frac{16\sigma^{**}}{3kk^*} \frac{T_\infty^3}{(\rho c_p)} \left(\frac{\partial^2 T}{\partial z^2} \right) + \frac{\mu}{(\rho c_p)} \left(\frac{\partial u}{\partial z} \right)^2 + \frac{Q^*}{(\rho c_p)} \exp(-n\nu_f^{-0.5}\Omega^{0.5}z)(T - T_\infty) \quad (3)$$

$$\left. \begin{aligned} \mu \frac{\partial u}{\partial z} = \frac{\partial \sigma}{\partial r} = \frac{\partial \sigma}{\partial T} \frac{\partial T}{\partial r}, \quad w = 0, \quad T = T_0 = T_\infty + T_{const} r^2, \quad \text{at } z = 0, \\ u \rightarrow 0, \quad T \rightarrow T_\infty, \quad \text{at } z = \infty \end{aligned} \right\} \quad (4)$$

Here $[r, z]$ are cylindrical coordinates, $\mu, \rho, \sigma^*, \beta_1, \beta_2, g, (u, v, w), \sigma^{**}, k^*, c_p, T, k, T_\infty, n, \sigma$ represent dynamic viscosity, density, electrical conductivity, linear and nonlinear thermal convections, gravity, velocity vector, Stefan-Boltzman constant, mean absorption coefficient, specific heat of nanofluid, temperature, thermal conductivity, external flow temperature, exponential constant, temperature constant, surface tension and $\sigma = \sigma_0 - \gamma_T(T - T_\infty)$ where γ_T is $\left(-\frac{\partial \sigma}{\partial T} \right) \Big|_{T=T_\infty}$.

Considering

$$u = r\Omega f, \quad v = \sqrt{\nu\Omega}h, \quad \theta(\xi) = \frac{T - T_\infty}{Ar^2}, \quad \xi = z\sqrt{\frac{\Omega}{\nu}} \quad (5)$$

We arrive

$$2f + h' = 0 \quad (6)$$

$$f'' - hf' - f'^2 - Mf' + \lambda\theta(1 + \beta_1\theta) = 0 \quad (7)$$

$$\frac{1}{Pr}(1 + R)\theta' - 2f\theta - h\theta' + QExp[-n\xi] + Ecf'^2 = 0 \quad (8)$$

$$h(0) = 0, \quad f'(0) = -2Ma, \quad \theta(0) = 1, \quad f'(\infty) = 0, \quad \theta(\infty) = 0 \quad (9)$$

Note that $\lambda, Ma, M, R, Q, E_c, \beta_i$, and Pr highlight mixed convection parameter, Marangoni number, Hartmann number, radiation parameter, heat generation parameter, Eckert number, nonlinear thermal convection parameter and Prandtl number.

Mathematically these variables are

$$\left. \begin{aligned} \lambda \left(= \frac{g\beta_1(T_0 - T_\infty)}{r\Omega^2} \right), \quad Ma \left(= \frac{\gamma_T Ax}{\mu\Omega} \right), \quad Pr \left(= \frac{\nu_f}{\alpha_f} \right), \quad M \left(= \frac{\sigma B_0^2}{\rho\Omega} \right), \\ R \left(= \frac{16\sigma^{**}T_\infty^3}{3kk^*} \right), \quad Q \left(= \frac{Q^*}{(\rho c_p)\Omega} \right), \quad Ec \left(= \frac{(r\Omega)^2}{c_{p1}(T_0 - T_\infty)} \right) \\ \beta_i \left(= \frac{\beta_2(T_0 - T_\infty)}{\beta_1} \right) \end{aligned} \right\} \quad (10)$$

Mathematically, entropy generation in presence of thermal radiation and Joule heating is addressed as

$$S_G = \frac{k}{T_\infty^2} \left(1 + \frac{16\sigma^{**}T_\infty^3}{3k^*k} \right) \left(\frac{\partial T}{\partial z} \right)^2 + \frac{\mu}{T_\infty} \left(\frac{\partial u}{\partial y} \right)^2 + \frac{\sigma^* B_0^2}{T_\infty} u^2 \quad (11)$$

dimensionless form is

$$N_G = (1 + R)\theta'^2 + Brf'^2 + BrMf^2 \quad (12)$$

The Bejan number which is the ratio of heat transport to total entropy is

$$Be = \frac{(1 + R)\theta'^2}{Brf'^2 + BrMf^2} \quad (13)$$

where $Br \left(= \frac{\mu(r\Omega)^2 T_\infty}{kA^2 r^4} \right)$ and $N_G \left(= \frac{S_G T_\infty^2 \nu}{kA^2 r^4} \right)$ signify the Brinkman number and entropy generation rate.

3. Physical description

This section is dedicated to analyze the trends of velocity, temperature, entropy generation and Bejan number via involved pertinent parameters. For this purpose Figs. (1–14) are constructed.

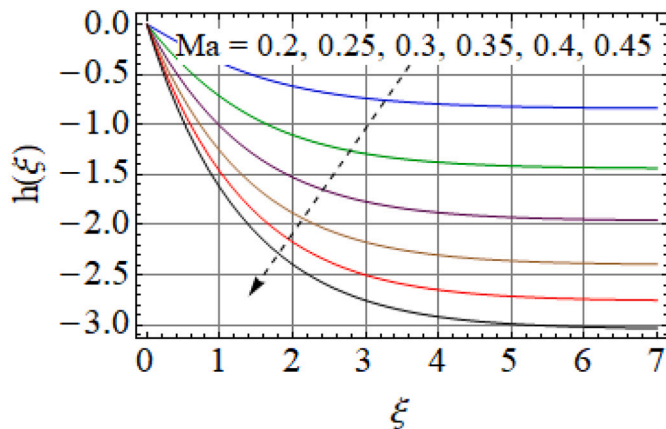


Fig. 1. $h(\xi)$ versus Ma .

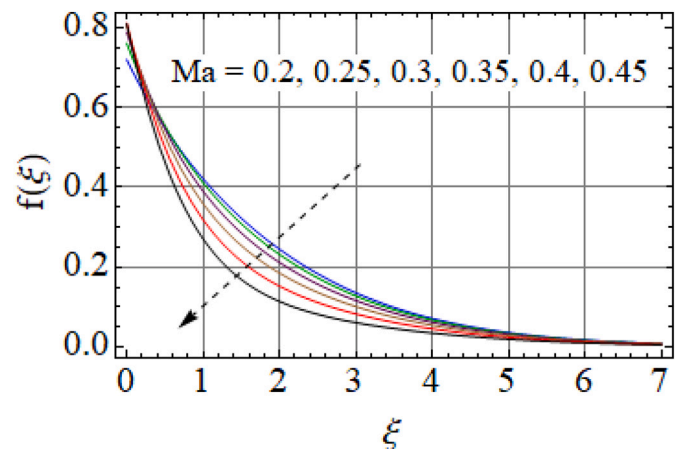


Fig. 2. $f(\xi)$ versus Ma .

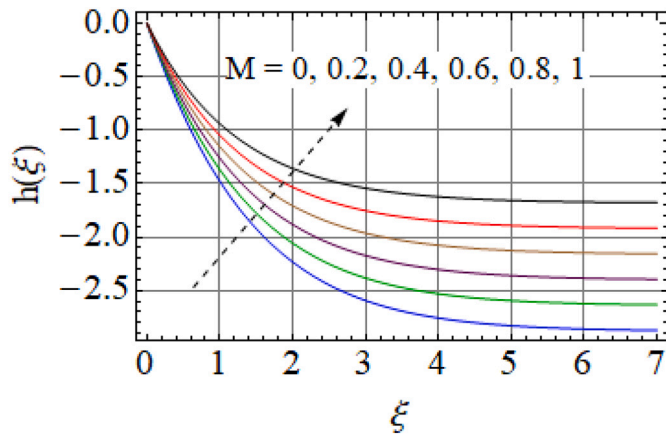


Fig. 3. $h(\xi)$ versus M .

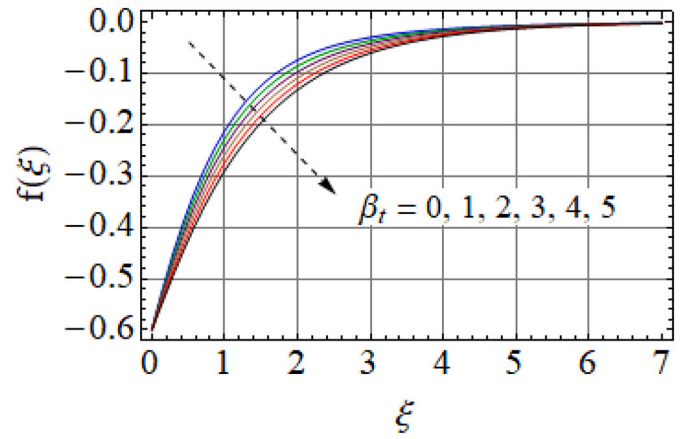


Fig. 6. $f(\xi)$ versus β_t .

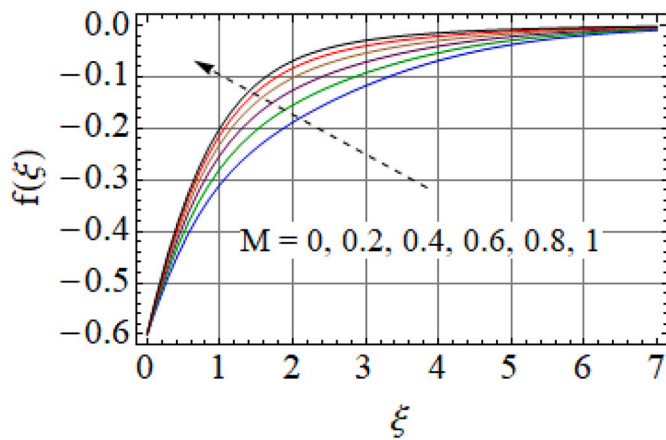


Fig. 4. $f(\xi)$ versus M .

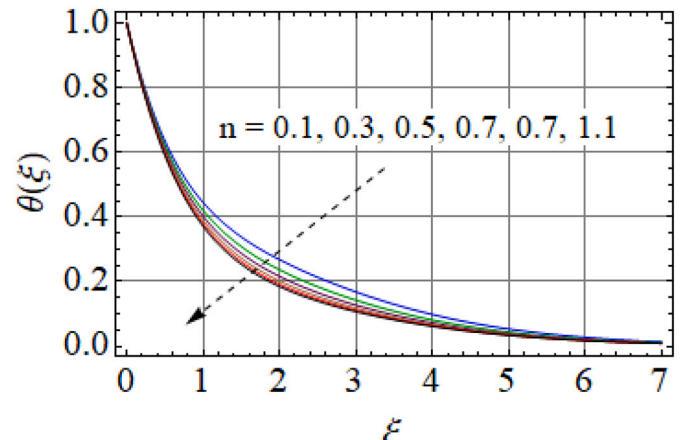


Fig. 7. $\theta(\xi)$ versus n .

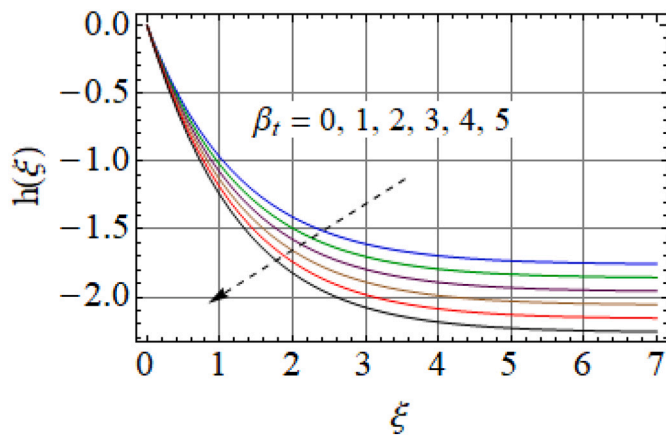


Fig. 5. $h(\xi)$ versus β_t .

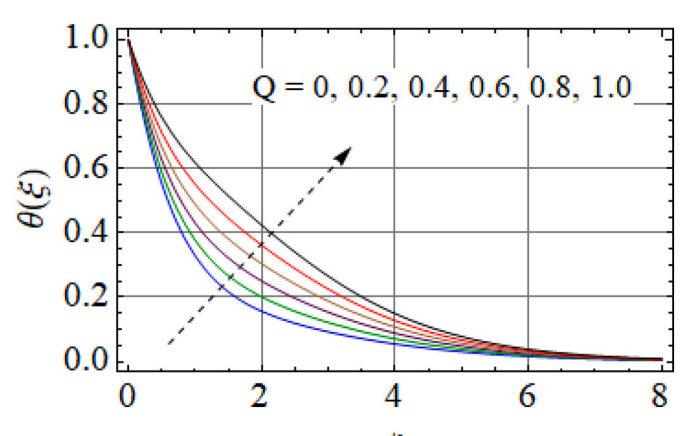


Fig. 8. $\theta(\xi)$ versus Q .

3.1. Velocity

For detail analysis of velocity profiles ($h(\xi)$, $f(\xi)$) against pertinent parameters Figs. (1–6) are constructed. Figs. 1 and 2 deal with the effect of Marangoni number against axial and radial velocity profiles. Axial velocity ($f(\xi)$) enhances for higher variation of Marangoni number ($Ma = 0.2, 0.25, 0.3, 0.35, 0.4, 0.45$) while radial velocity decreases. With increase in (Ma) surface tension increases due to which momentum boundary layer thickness and axial velocity rises. Figs. 3 and 4

demonstrate the features of axial and radial velocity profile against Hartmann number. It is seen that magnitude of axial and radial velocity profile decays for higher estimation of (M) Hartmann number is a increasing function of Lorentz force. With increase in (M) Lorentz force increases due to which resistance between the fluid particles enhances hence velocity decays for both axial and radial direction. Figs. 5 and 6 examine the trend of axial and radial velocity profile against nonlinear thermal convection parameter (β_t). Here ($h(\xi)$, $f(\xi)$) rises for greater

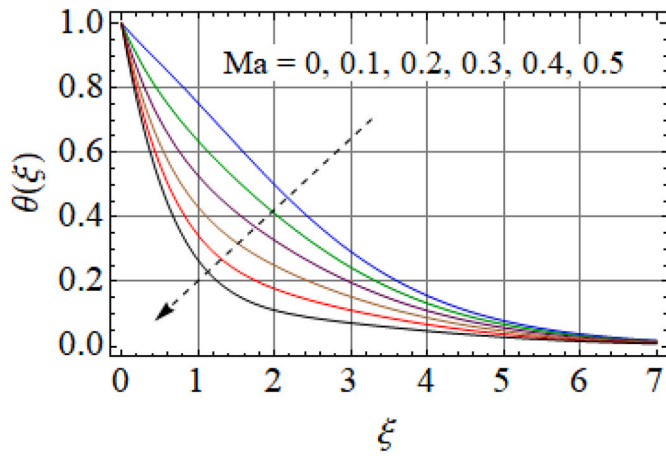


Fig. 9. $\theta(\xi)$ versus Ma .

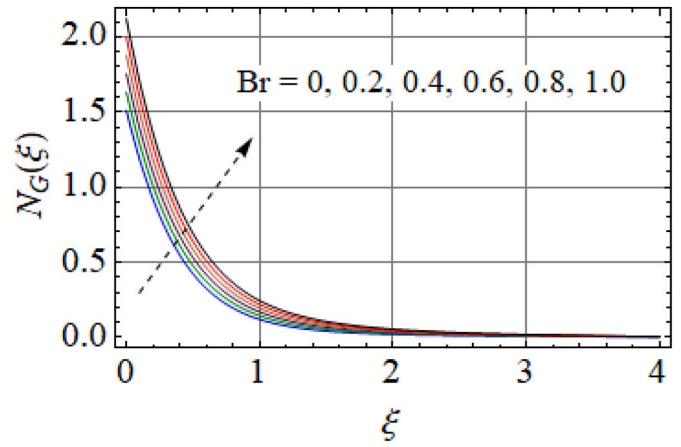


Fig. 12. $N_G(\xi)$ versus Br .

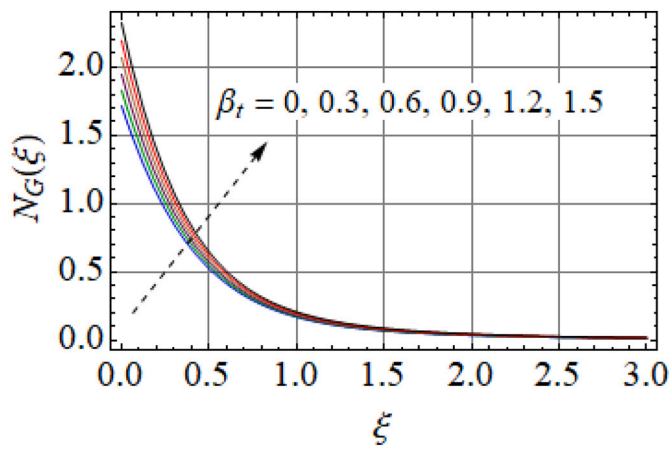


Fig. 10. $N_G(\xi)$ versus β_t .

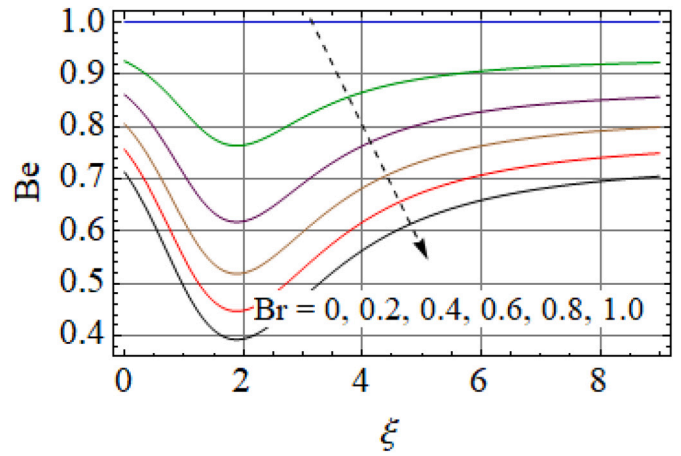


Fig. 13. Be versus Br .

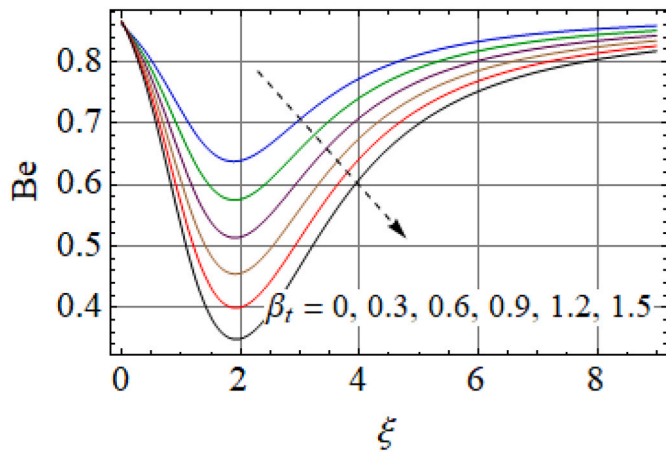


Fig. 11. Be versus β_t .

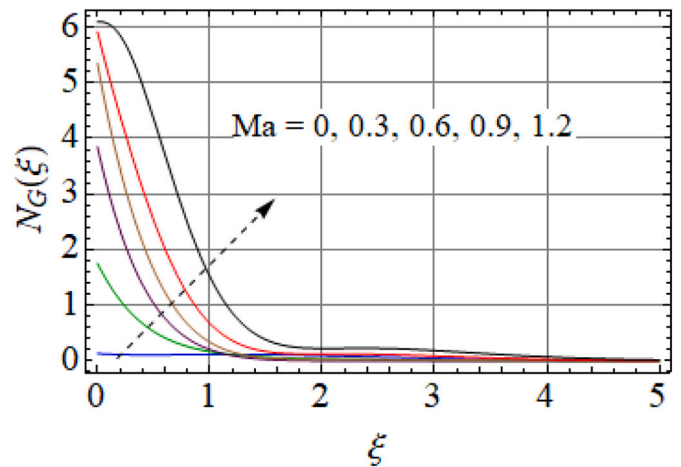


Fig. 14. $N_G(\xi)$ versus Ma .

estimations of (β_t) . With increase in values of (β_t) temperature difference between disk and ambient rises due to which velocity boosts up.

3.2. Temperature

Impact of exponential index (n) , heat generation parameter (Q) and Marangoni number (Ma) on temperature field is seen in Figs. (7–9). Here

temperature of the fluid decay with increment of (n) because n is negative power of exponential due to which heat generation effect starts decreasing drastically. Fig. 8 describes the variation of $(\theta(\xi))$ against heat generation parameter (Q) . Temperature of the fluid enhances via larger (Q) . Marangoni number effect on temperature is depicted in Fig. 9. Temperature of the fluid decays for higher Ma . With increase in (Ma) surface tension increases it means that temperature is decreasing

and strong force of attraction exist between surface and molecules.

3.3. Entropy and Bejan number

Figs. 10 and 11 delineate the impact of nonlinear thermal convection parameter (β_t) on entropy generation and Bejan number (Be). Here one can see that entropy of the system is increasing with respect to (β_t). It is due to the fact that temperature difference rises with increase in (β_t) due to which total entropy of the system enhances (See Fig. 10). On the other hand Bejan number decays for higher estimation of (β_t). It means that heat transfer irreversibility effect are less than viscous dissipation irreversibility effect (See Fig. 11). Figs. 12 and 13 describe the influence of Brinkman number (Br) against entropy generation and Bejan number. It is due to the fact that viscosity is in direct relation with (Br) so when viscosity of the fluid enhances resistance produces due to which disorderedness in the system increases (See Fig. 12). Fig. 13 shows that Bejan number decays for larger values of (Br). It shows that viscous dissipation irreversibility is prominent over heat transfer irreversibility (See Fig. 14). Fig. 14 shows the impact of Marangoni number (Ma) against entropy generation. Here we can see that entropy of the fluid rises due to increase in (Ma).

4. Conclusions

Important results of present study are mentioned below:

- Axial and radial velocities show increasing trend via Marangoni number and nonlinear thermal mixed convection parameter.
- Temperature decays via Q and n .
- Entropy generation boosts up for greater Br , β_t and Ma .
- Bejan number decays for Br and β_t .

Data availability

The data that support the findings of this study are available within the article, the data are made by the authors themselves and do not involve references of others.

Declaration of Competing Interest

The authors declare that they have no known competing financial interests or personal relationships that could have appeared to influence the work reported in this paper.

References

- [1] Y.H. Gangadharaiah, Double diffusive Marangoni convection in superposed fluid and porous layers, *Int. J. Innov. Res. Sci. Eng. Technol.* 2 (2013) 2625–2633.

- [2] P. Sreenivasulu, N.B. Reddy, M.G. Reddy, Effects of radiation on MHD thermosolutal Marangoni convection boundary layer flow with joule heating and viscous dissipation, *Int. J. Appl. Math. Mech.* 9 (2013) 47–65.
- [3] B. Mahanthesh, B.J. Gireesha, Thermal Marangoni convection in two-phase flow of dusty Casson fluid, *Results Phys.* 8 (2018) 537–544.
- [4] B. Mahanthesh, B.J. Gireesha, Scrutinization of thermal radiation, viscous dissipation and joule heating effects on Marangoni convective two-phase flow of Casson fluid with fluid-particle suspension, *Results Phys.* 8 (2018) 869–878.
- [5] T. Hayat, M. Ijaz Khan, M. Farooq, A. Alsaedi, T. Yasmeen, Impact of Marangoni convection in the flow of carbon-water nanofluid with thermal radiation, *Int. J. Heat Mass Transf.* 106 (2017) 810–815.
- [6] B. Mahanthesh, B.J. Gireesha, N.S. Shashikumar, S.A. Shehzad, Marangoni convective MHD flow of SWCNT and MWCNT nanoliquids due to a disk with solar radiation and irregular heat source, *Phys. E: Low-Dimens. Syst. Nanostruct.* 94 (2017) 25–30.
- [7] Y.J. Zhuang, Q.Y. Zhu, Numerical study on combined buoyancy–Marangoni convection heat and mass transfer of power-law nanofluids in a cubic cavity filled with a heterogeneous porous medium, *Int. J. Heat Mass Transf.* 71 (2018) 39–54.
- [8] T.S. Wang, W.Y. Shi, Influence of substrate temperature on Marangoni convection instabilities in a sessile droplet evaporating at constant contact line mode, *Int. J. Heat Mass Transf.* 131 (2019) 1270–1278.
- [9] T.N. Le, Y.L. Lo, Effects of sulfur concentration and Marangoni convection on melt-pool formation in transition mode of selective laser melting process, *Mater. Des.* 1795 (2019) 107866.
- [10] M. Qasem, N. Al-Mdallal, B. Indumathi, Ganga, A.K. Abdul Hakeem, Marangoni radiative effects of hybrid-nanofluids flow past a permeable surface with inclined magnetic field, *Case Stud. Therm. Eng.* (2020), 100571.
- [11] T. Hayat, M.I. Khan, S. Qayyum, A. Alsaedi, Entropy generation in flow with silver and copper nanoparticles, *Colloid Surf. A* 539 (2018) 335–346.
- [12] S.P. Goqo, S.D. Oloniju, H. Mondal, P. Sibanda, S.S. Motsa, Entropy generation in MHD radiative viscous nanofluid flow over a porous wedge using the bivariate spectral quasi-linearization method, *Case Stud. Therm. Eng.* 12 (2018) 774–788.
- [13] M.I. Khan, S.A. Khan, T. Hayat, M.I. Khan, A. Alsaedi, Nanomaterial based flow of Prandtl-Eyring (non-Newtonian) fluid using Brownian and thermophoretic diffusion with entropy generation, *Comput. Methods Prog. Biomed.* 180 (2019) 105017.
- [14] M.R. Salimi, M. Taeibi-Rahni, H. Rostamzadeh, Heat transfer and entropy generation analysis in a three-dimensional impinging jet porous heat sink under local thermal non-equilibrium condition, *Int. J. Therm. Sci.* 153 (2020) 106348.
- [15] S. Farooq, M.I. Khan, A. Riahi, W. Chammam, W.A. Khan, Modeling and interpretation of peristaltic transport in single wall carbon nanotube flow with entropy optimization and Newtonian heating, *Comput. Methods Prog. Biomed.* 192 (2020) 105435.
- [16] T. Hayat, M.I. Khan, T.A. Khan, M.I. Khan, S. Ahmad, A. Alsaedi, Entropy generation in Darcy-Forchheimer bidirectional flow of water-based carbon nanotubes with convective boundary conditions, *J. Mol. Liq.* 265 (2018) 629–638.
- [17] M. Rashid, M.I. Khan, T. Hayat, M.I. Khan, A. Alsaedi, Entropy generation in flow of ferromagnetic liquid with nonlinear radiation and slip condition, *J. Mol. Liq.* 276 (2019) 441–452.
- [18] M. Kiyasatfar, Convective heat transfer and entropy generation analysis of non-Newtonian power-law fluid flows in parallel-plate and circular microchannels under slip boundary conditions, *Int. J. Therm. Sci.* 128 (2018) 15–27.
- [19] M.I. Khan, A. Kumar, T. Hayat, M. Waqas, R. Singh, Entropy generation in flow of Carreau nanofluid, *J. Mol. Liq.* 278 (2019) 677–687.
- [20] P. Rana, N. Shukla, Entropy generation analysis for non-similar analytical study of nanofluid flow and heat transfer under the influence of aligned magnetic field, *Alexandria Eng. J.* 57 (2018) 3299–3310.
- [21] S.Z. Abbas, M.I. Khan, S. Kadry, W.A. Khan, M. Israr-Ur-Rehman, M. Waqas, Fully developed entropy optimized second order velocity slip MHD nanofluid flow with activation energy, *Comput. Methods Prog. Biomed.* 190 (2020) 105362.
- [22] R. Naz, M. Noor, Z. Shah, M. Sohail, P. Kumam, P. Thounthong, Entropy generation optimization in MHD pseudoplastic fluid comprising motile microorganisms with stratification effect, *Alexandria Eng. J.* 59 (2020) 485–496.